

Magnetic confinement and the sharp tachopause

MICHAEL E. McINTYRE

*Centre for Atmospheric Science at the
Department of Applied Mathematics and Theoretical Physics,
Centre for Mathematical Sciences, Wilberforce Road, Cambridge CB3 0WA, UK,
<http://www.atm.damtp.cam.ac.uk/people/mem/>*

Final preprint before copy editing, January 2006. Published version is Chapter 8 of *The Solar Tachocline*, ed. D. W. Hughes, R. Rosner & N.O. Weiss, Cambridge University Press, 2007) pp. 183–212. The line below Eq. (8.6) is correct in the *present* version.

Abstract

The discovery by Spruit of a new small-scale turbulent dynamo has significantly changed the tachocline model proposed by Gough and McIntyre (GM98). The small-scale dynamo is shear driven, is characteristic of stably stratified flows, and is mediated by the kink or ‘tipping’ instability elucidated for such flows by R. J. Tayler. The dynamo works best in high latitudes and supports turbulent Maxwell stresses large enough to dominate the angular momentum transport, taking over from the pure mean meridional circulation (MMC) proposed in GM98. What survives from the GM98 tachocline scenario is the laminar thermomagnetic boundary layer at the tachopause, essential for the confinement of the interior field \mathbf{B}_i by high-latitude downwelling. That downwelling is, however, itself confined within a double boundary layer at the tachopause. The thermomagnetic boundary layer sits just underneath a modified Ekman layer, in which the turbulent Maxwell stress of the small-scale dynamo diverges.

The effects of compositional stratification in the helium settling layer under the tachopause are considered. It is concluded that GM98’s “polar pits” to burn lithium are dynamically impossible and that the tachopause is not only sharp but globally horizontal. That is, the tachopause, as marked by the top of the helium settling layer, follows a single heliopotential to within a very tiny fraction of a megametre from equator to pole. Therefore the stably-stratified tachocline, defined in high latitudes as the layer of dynamically significant shear beneath the convection zone, must be thick enough to burn lithium. This is consistent with the helioseismic evidence because the high-latitude shear, even though crucial to the maintenance of the dynamo action, is held down in magnitude, by the dynamo’s turbulent Maxwell stresses, to values too small to be visible.

8.1 Introduction

Following Spiegel & Zahn (1992) and others, I start from the assumption that the fluid dynamics of the tachocline is a multi-timescale problem. Specifically, in order to understand the structure of the present tachocline I assume, and will argue in what follows, that one has to consider fluid-dynamical processes over the full range of timescales from the gigayear or secular timescale of solar evolution to the months and years of convection-zone overshoot and upper-tachocline MHD instabilities and turbulence, all touched on in the other chapters herein. That many timescales are important should hardly need saying, but does, perhaps, need saying here if only to counter the false dichotomy “slow versus fast” that seems to have taken hold in the literature. Indeed it seems possible, now, that even so basic a quantity as the tachocline thickness Δ may depend on the gigayear-timescale history, as well as on a variety of turbulent processes over a large range of timescales.

In what follows I assume it unnecessary to repeat my old arguments (1994, 2003a) against the Spiegel–Zahn horizontal-eddy-viscosity hypothesis — which arguments, in turn, point toward the inevitable existence of a global-scale magnetic field \mathbf{B}_i in the radiative interior, whether of fossil or dynamo origin (Gough & McIntyre 1998, hereafter GM98), as the only way to account not only for the interior’s solid rotation but also for the smallness of Δ , at most several tens of megametres according to helioseismology (Chapter 3 & refs.). The argument for inevitability still seems significant in itself, given the far greater uncertainties about the origin, and the viability, of magnetic fields in the radiative interior. There, the gigayear-timescale escapology of magnetic fields has Houdini-like possibilities (see Chapter 11) involving the nonlinear effects of instabilities and Parker flux-tube buoyancy in combination.

The argument for inevitability of a magnetic interior can be summarized in two parts. First, a nonmagnetic interior cannot be held in solid rotation by real stratified, layerwise-two-dimensional turbulence. Such turbulence, if it were to be excited, would tend to be “anti-frictional” — to drive the system away from solid rotation and not toward it (McIntyre 1994, 2003a,b & refs.). The effect would be qualitatively unlike that of the hypothesized horizontal eddy viscosity. Second, a nonmagnetic interior would be incapable of withstanding another fluid-dynamical process that would also drive it away from solid rotation and that would, furthermore, as originally pointed out by Spiegel and Zahn (1992), make Δ values significantly larger than permitted by the helioseismic evidence. That process — the downward “radiative spreading” or “Haynes–Spiegel–Zahn burrowing”, into a nonmagnetic inte-

rior, of mean meridional circulations (MMCs) and differential rotation — will be revisited here together with the concomitant notion of “gyroscopic pumping”. As well as making Δ values too large, the downward-burrowing MMCs would prevent a helium settling layer from forming at the top of the interior, as well as probably burning too much beryllium.

The arguments against nonmagnetic horizontal eddy viscosity will prove robust, I believe, (a) because of their clearcut basis in the fundamental principles of nonmagnetic, stratification-constrained eddy motion, especially potential-vorticity conservation and invertibility (e.g. McIntyre 2003a,b & refs.), and (b) because of the comprehensive testing and vindication of those fundamental principles by high-resolution observations and modelling of, especially, the Earth’s stratosphere.† So the main focus of this chapter will not be on those arguments, but rather on how, if the existence of the global-scale interior \mathbf{B}_i is accepted as practically certain, the GM98 scenario now needs to be modified in the light of advances in our knowledge of MHD turbulence. The focus is not now on asking *whether* it is a global-scale \mathbf{B}_i that limits Δ , but on understanding more clearly *how* it does so. The MHD-turbulent aspects will force a reexamination of how azimuthal stresses are supported between the interior and the overlying turbulent layers, and how they fit in with the contributions of MMCs to angular momentum exchange.

Despite radical changes, one important feature of the GM98 scenario seems to have survived so far, with a little help from Occam’s razor. This is the prediction of a ventilated (helium-poor) tachocline terminated by a sharp tachopause, across which there is a strong jump in compositional or heavy-element abundance gradients, from zero in the tachocline to a finite value in the helium settling layer just beneath, corresponding to a contribution N_μ^2 to the buoyancy frequency squared that is a significant fraction of the typical thermal value $N^2 \sim 10^{-6} \text{ s}^{-2}$. This points toward the validity of helioseismic calibrations of the kind attempted in Elliott & Gough (1999).

A feature that does not, on the other hand, survive from GM98 in any form at all is the large-scale, laminar, field-free ($\mathbf{B} \equiv 0$) downwelling throughout high latitudes, occupying a substantial fraction of the thickness of the tachocline. The original GM98 scenario relied entirely on Reynolds and Maxwell stresses in the convection zone to produce (by gyroscopic pumping) the downwelling MMC needed (a) to confine the interior field \mathbf{B}_i in high lati-

† A striking observational example visible to any web browser, illustrating the detail in which the stratosphere is now observed, can be quickly found by googling “gyroscopic pump in action”. This is an animated version of figure 8.1, p. 121, of McIntyre (2003a), courtesy of the Wuppertal remote-sensing group. There is a vast literature of published papers in leading journals; see for instance Manney *et al.* (1994), Riese *et al.* (2002). See also www.atm.damtp.cam.ac.uk/people/mem/papers/ECMWF/ecmwf05.html

tudes as well as (b) to transfer angular momentum as necessary and (c) to ventilate the tachocline. But the hypothesis of large-scale field-free downwelling in high latitudes, pumped entirely by convection-zone stresses, is now untenable — whether or not we include overshoot-layer stresses — because it has been convincingly shown by Spruit (1999, 2002, hereafter S99, S02), building on the classic work of R. J. Tayler in the 1970s, that most if not all of the high-latitude downwelling region, even if initially field-free, could not remain so. Because of its vertical shear, the region would be MHD-unstable in such a way as to evolve into a small-scale dynamo.

The dynamo action is mediated by what S99 and S02 conveniently call a ‘Tayler instability’ — a stratification-modified pinch or kink-type (‘tipping’) instability — of the toroidal field wound up by the shear, on large horizontal scales but on radial scales small enough for thermal diffusion to counteract the stable stratification. The ability of the Tayler instability to close the dynamo loop has been verified by numerical experiments (Braithwaite & Spruit 2006). This small-scale dynamo seems likely to be most effective in latitudes within the poleward half of the range, and possibly also in some lower-latitude band or bands not too close to the equator.

The implication (§8.4) turns out to be that the MMC, or at least the high-latitude downwelling branch most critically needed to confine \mathbf{B}_i , is gyroscopically pumped by turbulent Maxwell stresses that diverge not in the convection zone or overshoot layer but, rather, near the base of an MHD-turbulent tachocline. This region will be referred to as the *lowermost tachocline* in high latitudes. The orders of magnitude dictate that the stress divergence and consequent MMC are confined to within a fraction of a megametre of the tachopause, where a double boundary-layer structure must exist. The turbulence and gyroscopic pumping could be continuous or intermittent, depending on $|\mathbf{B}_i|$ values.

Before developing these ideas it is necessary to deal with one fundamental question that was raised at the Workshop. GM98’s inevitability argument and its further developments just sketched rely, of course, on the physical reality of the gyroscopic-pumping and burrowing mechanisms for MMCs penetrating a nonmagnetic interior. Those mechanisms are well understood and have been carefully studied. They show up most plainly in thought-experiments in which the Reynolds and Maxwell stress divergences in the overlying turbulent layers are replaced by an artificially prescribed, azimuthally symmetric, azimuthally directed force field \bar{F} (Haynes *et al.* 1991). If that force field pushes fluid retrogradely, for instance, then the Coriolis effect tries to turn the fluid poleward. As detailed analysis confirms, this amounts to a systematic mechanical pumping action that drives

MMCs. Ekman pumping is the special case in which the force happens to be frictional. But any azimuthal force will do, hence the generic term “gyroscopic pumping”. Persistent gyroscopic pumping in some layer of any stratified, rotating, thermally relaxing and *nonmagnetic* system with a finite pressure scale height generates MMCs that continually burrow downward. This was first clearly shown in the detailed, and complementary, independent investigations by Haynes *et al.* (1991) and Spiegel & Zahn (1992). The burrowing mechanism is so fundamental — to any attempt to understand the tachocline and to assess magnetic versus non-magnetic scenarios — that I find it convenient to give the mechanism a distinctive name, “Haynes–Spiegel–Zahn burrowing” or “HSZ burrowing” for brevity, whenever verbal precision is necessary.†

The question raised at the Workshop was whether HSZ burrowing is a real physical phenomenon. It was claimed, in effect, that the two studies just cited are qualitatively in error and that there is no such thing as HSZ burrowing, even in the absence of the interior magnetic field \mathbf{B}_i . The claim was based on a recent study of MMCs using nonmagnetic equations (Gilman & Miesch 2004, hereafter GMi) whose results appear to imply that MMCs driven from above cannot penetrate downward more than a negligible distance, probably less than the vertical resolution of helioseismic inversions. If that were correct then most of the arguments in this chapter, and in its predecessors including GM98, would fail utterly. Therefore §8.2 revisits the problem studied in GMi, using the same formulation and notation. It turns out that through a quirk of formulation the solutions obtained in GMi make up an incomplete set. They are a special subset of solutions, *for each of which the gyroscopic pumping exactly vanishes at each latitude*. No gyroscopic pumping implies no burrowing! There is, after all, no conflict. Indeed the analysis in §8.2, based on an idealized slab model, provides the simplest possible illustration of the pumping and burrowing mechanisms, supplementing the original analytical and numerical work of Haynes *et al.* (1991) and Spiegel & Zahn (1992).

§8.3 goes on to argue that turbulence in the interior, below the tachopause, must be exceedingly sporadic. Thus, within the gigayear perspective a random snapshot of the Sun is almost certain to show an interior that is entirely laminar or very nearly so. Broadly speaking this is consistent with the standard solar modelling assumption of a microscopically diffusive helium settling layer, though it remains possible that the layer is somewhat

† As already mentioned it has also been called “spreading” but, with the Sun’s gravitational field pulling hard on my imagination, I prefer “burrowing” because it unambiguously connotes downwardness.

thickened, and indeed its heavy-element contrast somewhat increased, by the sporadic interior mixing.

§8.4 examines what S02’s arguments then imply about tachocline and tachopause structure and high-latitude downwelling. As already mentioned, such downwelling is critical to the confinement of \mathbf{B}_i , a point underlined by recent numerical studies (Garaud 2002; Braithwaite & Spruit 2004; Brun & Zahn 2006) showing the tendency for the poloidal part of an internal dipolar field to diffuse its lines upward and outward through a substantial high-latitude region. That tendency is, however, easily held in check by the downwelling within the double-boundary-layer structure of the lowermost tachocline. Thus the double boundary layer appears well able to confine \mathbf{B}_i in high latitudes.

Intriguingly if frustratingly, the mean shears within the double boundary layer turn out to be far too small to be helioseismically visible. Moreover, the same appears true of shears throughout the bulk of the high-latitude, stably-stratified tachocline. Therefore the visible shear must, in high latitudes, reside wholly in the lower convection zone and overshoot layer. As will be seen shortly this is consistent with the helioseismic evidence. A similar situation may be expected in any low-latitude band that goes turbulent via the shear driven, Tayler-mediated small-scale dynamo action, though, even if such a band exists, the properties of the Tayler instability — favoured by a poleward decrease in the toroidal field wound up by the shear — suggest that the band would have limited latitudinal extent. It might also exhibit unsteady behaviour, such as a life cycle involving poleward migration on timescales perhaps $\sim 10^6$ y or more.

§8.5 extends the idealized analysis of §8.2 to allow for compositional gradients in the underlying helium settling layer, in order to reassess GM98’s “lithium-burning polar pit” hypothesis. It appears that N_μ values, acting in concert with the surrounding \mathbf{B}_i , are more than enough to inhibit the formation of such pits and, indeed, to constrain the tachopause — defined as the bottom of the ventilated layer, equivalently the top of the helium settling layer — to be very close to the horizontal.

Moreover, this constraint on tachopause slope holds tightly even on a global scale. It appears that the tachocline, assuming it is sufficiently ventilated, must have not only an approximately constant chemical composition but also constant depth over all latitudes. More precisely, the tachopause has to follow an effective gravitational–centrifugal potential, globally, to within a very tiny fraction of a megametre.

If this picture is anywhere near correct then the only way to burn lithium is simply for Δ , defined in terms of tachopause depth, to be large enough.

A careful lithium-burning modelling study by Christensen-Dalsgaard *et al.* (1992) suggests a need for Δ values close to 65 Mm measured downwards from the helioseismic bottom of the convection zone at $0.713R_{\odot}$. This puts the tachopause at $0.62R_{\odot}$. If one superposes the $0.62R_{\odot}$ circle on to Figure 3.7 of Chapter 3, then especially in high latitudes one sees what looks like a substantial shear-free region beneath the overshoot layer, consistent with the earlier statement that the visible shear must, in high latitudes, reside wholly in the lower convection zone and overshoot layer. This of course is very different from the GM98 scenario. §8.6 offers some concluding remarks, mainly on some uncertainties regarding tachocline ventilation.

It might be thought that the terminology should be changed if, as I am now suggesting, the ventilated tachocline is distinctly deeper than the tachocline defined by shears visible in a helioseismic inversion. But observational invisibility does not imply dynamical insignificance. And indeed, in the scenario to be developed, the invisible shear has a crucial role in the high-latitude dynamics and ventilation of the tachocline, all the way down to the tachopause — defined, as here, to mean the ventilated layer and its lower boundary, or equivalently the top of the helium settling layer.

8.2 Gyroscopic pumping and HSZ burrowing

Consider the thought experiment of Haynes *et al.* (1991), performed on GMi's nonmagnetic, linearized Cartesian slab model. We take coordinates (x, y, z) respectively eastward, northward and upward as in GMi, with corresponding velocity components (u, v, w) and Coriolis vector idealized as $(0, 0, 2\Omega)$. For definiteness the top of the model, $z = z_{\text{top}}$ say, is taken to be isothermal, stress-free, and impermeable to mass. The prescribed azimuthal force field $\{\bar{F}(y, z), 0, 0\}$ is applied to an upper layer $z_f < z < z_{\text{top}}$. The force \bar{F} is assumed weak enough for linearization to remain valid. We ask to what extent the response to \bar{F} penetrates downward into the unforced region $z < z_f$, where we take the buoyancy frequency N of the stratification to be constant as in GMi. As in GMi we ignore compositional gradients, as would be an appropriate idealization if the interior were nonmagnetic and HSZ burrowing active over the gigayear timescale. For then no helium settling layer would have a chance to form (further discussion in §8.5), and the thermal stratification would dominate. Steady-state solutions of the type found in GMi should, of course, be valid in the unforced region.

The profile of N within the forcing layer $z_f < z < z_{\text{top}}$ will be left unspecified. In the original GM98 scenario, in which the forcing layer was identified as the convection zone, we would have $N \equiv 0$ for $z_f < z < z_{\text{top}}$. But there is no difficulty in including the overshoot layer, and indeed an entire turbulent

tachocline, as part of the forcing layer. The thought experiment is meant to imitate the effect of any overlying layer, stratified in any way, in which the turbulent Reynolds and Maxwell stresses in an x -averaged description diverge to give the force field $\bar{F}(y, z)$. Any such force field, arising from internal stresses, must have a domain integral that vanishes,

$$\iint \bar{F}(y, z) dy dz = 0 , \quad (8.1)$$

even though its vertical integral $\bar{\mathcal{F}}(y) = \int_{z_f}^{z_{\text{top}}} \bar{F}(y, z) dz$ need not vanish.

Again following GMi we use the Boussinesq equations and describe thermal relaxation toward radiative equilibrium by a constant thermal diffusivity $\kappa \approx 10^7 \text{ cm}^2 \text{ s}^{-1}$. Some aspects of the problem depend on non-Boussinesq effects, which in a doubly infinite domain select downward penetration at the expense of upward, as illustrated by Haynes *et al.*'s analysis. Here we have replaced those effects by the artifice of cutting off the fluid domain at $z = z_{\text{top}}$.

Defining the buoyancy-acceleration anomaly ϑ in the standard way as gravity times the fractional temperature anomaly on a pressure surface, $\vartheta = gT/\bar{T}$ in GMi's notation, we have, for axisymmetric dynamics $\partial/\partial x = 0$,

$$\frac{\partial v}{\partial y} + \frac{\partial w}{\partial z} = 0 , \quad (8.2a)$$

$$\frac{\partial u}{\partial t} - 2\Omega v - \nu \frac{\partial^2 u}{\partial z^2} = \bar{F}(y, z) , \quad (8.2b)$$

$$\frac{\partial^2 v}{\partial z \partial t} + 2\Omega \frac{\partial u}{\partial z} + \frac{\partial \vartheta}{\partial y} - \nu \frac{\partial^3 v}{\partial z^3} = 0 , \quad (8.2c)$$

$$\frac{\partial \vartheta}{\partial t} + N^2 w - \kappa \frac{\partial^2 \vartheta}{\partial z^2} = 0 . \quad (8.2d)$$

As in GMi we have included viscous terms, with constant momentum diffusivity ν . The third equation (8.2c) may be called the generalized thermal-wind equation. It is formed by eliminating the pressure between the hydrostatic equation and the vertical derivative of the meridional momentum equation. As is realistic for the solar tachocline we assume that Ω is effectively large (rapidly rotating system, small Rossby number), so that in (8.2c) there is a powerful tendency toward thermal-wind balance, $2\Omega \partial u/\partial z \approx -\partial \vartheta/\partial y$.

If a system like this is started from an undisturbed initial state with u , v , w , and ϑ all zero then, as Haynes *et al.* showed in an essentially similar problem, the typical behaviour within the forcing layer is robustly as follows. First, u accelerates in response to \bar{F} , followed by Coriolis turning of (u, v) . The system then approaches a locally steady or nearly-steady state

in which thermal-wind balance prevails, and in which $-2\Omega v$ has come into approximate balance with \bar{F} in Equation (8.2b). The effect of the ν term in (8.2b) is equivalent to a slight redistribution of \bar{F} , leaving the qualitative picture unaffected. The balance

$$-2\Omega v \approx \bar{F} \quad (8.3)$$

describes the persistent gyroscopic pumping of meridional flow v by the steady azimuthal force field \bar{F} . Note that $\bar{F} < 0$ implies $v > 0$, confirming that a retrograde force pumps fluid poleward.

Now GMi's results should apply to the unforced region $z < z_f$. GMi assume a steady state with $\bar{F} \equiv 0$, leading to a single equation that applies in the unforced region,

$$\frac{\partial^6 v}{\partial z^6} + \frac{4\Omega^2}{\nu^2} \frac{\partial^2 v}{\partial z^2} + \frac{N^2}{\nu\kappa} \frac{\partial^2 v}{\partial y^2} = 0. \quad (8.4)$$

(This comes from assuming N constant, taking $\partial^3/\partial z^3$ of (8.2c), then successively eliminating u , ϑ , and w .) GMi consider solutions of the form $v \propto e^{kz} \sin(y/\ell)$, where ℓ is a suitable latitudinal lengthscale and k is a complex constant satisfying the characteristic equation

$$k^6 + \frac{4\Omega^2}{\nu^2} k^2 - \frac{N^2}{\nu\kappa} \ell^{-2} = 0, \quad (8.5)$$

of whose six roots three correspond to downward evanescence. Consideration of the scale $(\text{Re}k)^{-1}$ for evanescence when the latitudinal lengthscale ℓ takes reasonable values $\sim 10^2$ Mm gives vertical scales of the order of a few tens of megametres at most, even when both ν and κ are both taken to have large eddy values $\sim 10^{12}$ cm²s⁻¹. Microscopic values give a small fraction of a megametre. If these were the only possible solutions then they would certainly imply what was claimed at the Workshop, namely that there is no such thing as HSZ burrowing into a nonmagnetic interior. GM98's inevitability argument would then fail.

Let us ask, however, what a boundary-layer solution of this kind in the unforced region $z < z_f$ would imply about the forcing function $\bar{F}(y, z)$ in the layer above. All variables are downward evanescent. Therefore, by integrating (8.2a) over all z and invoking the assumption that the upper boundary $z = z_{\text{top}}$ is impermeable to mass, we may deduce that the y derivative of $\int_{-\infty}^{z_{\text{top}}} v dz$ vanishes, so that

$$\int_{-\infty}^{z_{\text{top}}} v dz = C \quad (8.6)$$

where C is a constant. We have also assumed that the upper boundary is

stress-free, $\nu \partial(u, v)/\partial z = 0$. So integrating (8.2b) for the steady state gives

$$\bar{\mathcal{F}}(y) = \int_{z_f}^{z_{\text{top}}} \bar{F}(y, z) dz = -2\Omega \int_{-\infty}^{z_{\text{top}}} v dz = -2\Omega C. \quad (8.7)$$

Now this is compatible with (8.1) only if $C = 0$; therefore

$$\bar{\mathcal{F}}(y) = -2\Omega \int_{-\infty}^{z_{\text{top}}} v dz = 0 \quad (8.8)$$

at each y . In other words, there is no net gyroscopic pumping — no vertically integrated azimuthal force, and no vertically integrated meridional mass flux and volume flux in the boundary layer — at any y . GMi's solutions are all solutions for which the net gyroscopic pumping exactly vanishes at each y .

That fact is not obvious from GMi's perspective, in which only the unforced layer $z \leq z_f$ is considered. We may note, however, that all GMi's solutions satisfy the special relation $\nu \partial^2 u / \partial y \partial z = 2\Omega w$. This can be straightforwardly verified either from the solutions, or from the variant of (8.8) obtained by integrating (8.2b) from $-\infty$ to any $z \leq z_f$, noting that $\bar{F} = 0$. Even though it might appear that w is being arbitrarily prescribed at the top — and should therefore represent any gyroscopic pumping from above — the u field, invisible in GMi's formulation, has cunningly organized itself in such a way that the boundary $z = z_f$ exerts an azimuthal viscous stress on the fluid beneath that just cancels† the pumping effect of the prescribed w .

To double-check this we look at an explicit solution that includes the upper forcing layer $z_f < z < z_{\text{top}}$. For simplicity we set $N \equiv 0$ and $\bar{F} \propto \sin(y/\ell)$, independent of z within the forcing layer. Then within that layer we see that equations (8.2) admit a simple solution of the form $v = -\bar{F}/2\Omega$, with $u \propto \sin(y/\ell)$, both independent of z , the remaining variables being given by $\vartheta \equiv 0$ and $w = -(z_{\text{top}} - z)(d\bar{F}/dy)/2\Omega \propto (z_{\text{top}} - z) \cos(y/\ell)$. But a boundary-layer solution in which u is a continuous function of z satisfies (8.2b) at $z = z_f$ only if (consistently with $\nu \partial^2 u / \partial y \partial z = 2\Omega w$ for $z \leq z_f$) we add a delta function to \bar{F} whose strength is precisely $-(z_{\text{top}} - z_f)\bar{F}$. That is, to get a solution of GMi's boundary-layer form we must choose this extra contribution to \bar{F} such that the total force integrates to zero, $\bar{\mathcal{F}}(y) = 0$, as already seen from (8.8). For this particular solution we also need a delta-function heat source and sink $\propto \cos(y/\ell)$ at $z = z_f$, that is, where N^2 is discontinuous, but such an artifice does not affect the issue of gyroscopic pumping.

For the generic case in which $\bar{\mathcal{F}}(y)$ does not, by contrast, vanish, we

† The Spiegel–Zahn eddy viscosity similarly cancels the pumping from above, through horizontal rather than vertical transmission of azimuthal stress. In effect one has two gyroscopic pumps, an upper pump producing a certain mass flux, and a lower one negating it by producing an equal and opposite mass flux.

must expect to find additional solutions that do not have the boundary-layer character implied by (8.5). Even within the steady-state framework, we do not have to look far to find them. In place of (8.4) consider the corresponding equation for u . Substituting $v \propto \partial^2 u / \partial z^2$ from (8.2b), we have

$$\frac{\partial^8 u}{\partial z^8} + \frac{4\Omega^2}{\nu^2} \frac{\partial^4 u}{\partial z^4} + \frac{N^2}{\nu\kappa} \frac{\partial^4 u}{\partial y^2 \partial z^2} = 0, \quad (8.9)$$

with characteristic equation

$$k^8 + \frac{4\Omega^2}{\nu^2} k^4 - \frac{N^2}{\nu\kappa} \ell^{-2} k^2 = 0. \quad (8.10)$$

This has two more roots, both zero, signalling the existence of two extra solutions, $u = \text{constant}$ and $u \propto z$. So if we leave the y -origin arbitrary the general solution in the unforced region is

$$u = \left(\sum_1^6 C_j e^{k_j z} + C_7 + C_8 z \right) \sin(y/\ell), \quad (8.11)$$

where the k_j are the six roots of (8.5) and the C_j are arbitrary constants. Such solutions are applicable when, for instance, we take

$$\bar{\mathcal{F}}(y) = \mathcal{F}_0 \sin(y/\ell) \quad (8.12)$$

with constant \mathcal{F}_0 .

To see what (8.11) means physically, it is simplest to consider first a problem with an artificial lower boundary, say $z = 0$, far beneath the forcing layer, where far means many evanescence height scales $(\text{Re} k)^{-1}$. On $z = 0$ we impose $u = v = w = 0$ (impermeable and no-slip) and $\kappa \partial \vartheta / \partial z = 0$ (heat flux held to its background value). Then with $\bar{\mathcal{F}}(y) = \mathcal{F}_0 \sin(y/\ell)$ it is a straightforward exercise to prove that $C_7 = 0$ and $C_8 = \nu^{-1} \mathcal{F}_0$, with exponentially small error, and that the solution in the unforced region is

$$u = \left(\sum_{j=1}^3 C_j e^{k_j z} + \nu^{-1} \mathcal{F}_0 z \right) \sin(y/\ell) \quad (8.13)$$

where k_1, k_2, k_3 are the downward-evanescent roots of (8.5). They are needed to describe details within a thin layer near the top. Beneath that layer, we have $v = w = 0$ and $\vartheta = 2\Omega \ell \nu^{-1} \mathcal{F}_0 \cos(y/\ell)$. The upward-evanescent roots k_4, k_5, k_6 are absent because the solution just described satisfies the four lower boundary conditions as it stands, with exponentially small error. The coefficient of z , $C_8 = \nu^{-1} \mathcal{F}_0$, is determined regardless of details near the

top, because in the steady state (8.8) is replaced by

$$\bar{\mathcal{F}}(y) = \nu \frac{\partial u}{\partial z} \Big|_{z=0}. \quad (8.14)$$

This comes from integrating (8.2a) and (8.2b) from $z = 0$ to z_{top} then using (8.1) and the bottom boundary conditions. In order to have a steady state in this linear model, the net applied force $\bar{\mathcal{F}}$ must be balanced at each y by the stress on the bottom. This pins down the coefficient of z . The existence of the steady-state solution (8.13) is an easy way to see that, in the original time-dependent thought experiment, the influence of $\bar{\mathcal{F}}$ must have burrowed all the way to the bottom — regardless of how far down the bottom may be. If we take the bottom down toward $z = -\infty$ then the time to reach the steady state increases without bound.

Notice that this solution describes another situation in which the gyroscopic pumping has been cancelled by a viscous stress. Before that, as the burrowing proceeds, the pumping drives a MMC whose Coriolis force accelerates u values up to such extremes, $\propto \nu^{-1}$ when ν is considered small, that the viscous stress spanning the entire depth $0 < z < z_f$ comes into balance with the force applied to the overlying layer $z_f < z < z_{\text{top}}$. Of course such extremes could violate the original linearization. But the real significance of the foregoing is that the response to $\bar{\mathcal{F}}(y)$, in the *absence* of artificial lower boundary, must be inherently time-dependent as originally shown by HSZ.

On the long timescale of the burrowing process, and when $\kappa \gg \nu$, the time derivative in (8.2d) may be neglected as well as that in (8.2c), where, moreover, thermal-wind balance is an excellent approximation. So by taking $\partial^2/\partial y^2$ of (8.2b) and then successively eliminating v through (8.2a), w through (8.2d) with $\partial/\partial t$ neglected, then finally ϑ through thermal-wind balance $\partial\vartheta/\partial y = -2\Omega \partial u/\partial z$ in place of (8.2c), we get

$$\left(\frac{\partial}{\partial t} - \nu \frac{\partial^2}{\partial z^2} \right) \frac{\partial^2 u}{\partial y^2} - \frac{4\Omega^2 \kappa}{N^2} \frac{\partial^4 u}{\partial z^4} = \frac{\partial^2 \bar{F}}{\partial y^2}, \quad (8.15)$$

recovering Spiegel & Zahn's result that when thermal relaxation is diffusive and ν sufficiently small then the burrowing behaviour is hyperdiffusive, with hyperdiffusivity $4\Omega^2 \ell^2 \kappa / N^2$ for latitudinal lengthscale ℓ . This may be compared with Haynes *et al.*'s result in the Boussinesq limit, $H \rightarrow \infty$ in their notation: when the thermal relaxation is Newtonian with timescale $\kappa_{\text{Newt}}^{-1}$ then the burrowing behaviour is diffusive with diffusivity $4\Omega^2 \ell^2 \kappa_{\text{Newt}} / N^2$. Notice that the timescale for burrowing is sensitive to the latitudinal scale ℓ , behaving as ℓ^{-2} .

Before leaving this topic we note for completeness the steady-state solution of (8.2a)–(8.2d) that idealizes the GM98 laminar-downwelling scenario, within a nonmagnetic tachocline of nominal thickness $\Delta = z_f$ at the bottom of which, $z = 0$, there is a thermomagnetic boundary layer able to accept a certain volume flux $w_0 \cos(y/\ell)$, say, per unit area. That flux is governed by the magnitude of the global-scale interior field \mathbf{B}_i , and so the overlying layers must adjust themselves so as to pump exactly that much flux, which flux GM98 estimated to scale as $|\mathbf{B}_i|^{1/3}$.

With microscopic values of ν and κ we may take $\Delta \gg (\text{Re}k)^{-1}$. Then, apart from details near $z = z_f = \Delta$, the solution in $0 < z < \Delta$ is as follows. It confirms the GM98 result that, for given $u_{z=\Delta}$, $w_0 \propto \Delta^{-3}$ implying $\Delta \propto |\mathbf{B}_i|^{-1/9}$:

$$u = \frac{N^2 w_0}{24 \Omega \ell \kappa} z^2 (3\Delta - 2z) \sin(y/\ell), \quad (8.16a)$$

$$v = 0, \quad (8.16b)$$

$$w = w_0 \cos(y/\ell), \quad (8.16c)$$

$$\vartheta = \frac{N^2 w_0}{2\kappa} z (\Delta - z) \cos(y/\ell). \quad (8.16d)$$

The relation $w_0 \propto \Delta^{-3}$ follows from (8.16a) with $z = \Delta$. Also $\mathcal{F}_0 = -2\Omega\ell w_0$ in (8.12), from integrating (8.2a) and (8.2b) as before. Following GM98 we have assumed isothermal conditions $\vartheta = 0$ at $z = 0$ as well as at $z = z_{\text{top}}$, and $N \equiv 0$ in the forcing layer $z_f < z < z_{\text{top}}$ to make it into an idealized, exactly isothermal convection zone. The model tachocline described by (8.16) is frictionless, with angular momentum exchange across it mediated solely by the MMC and handed over to the Maxwell stress in the thermomagnetic boundary layer. GM98 estimated that $w \sim 10^{-5} \text{ cm s}^{-1}$, more than enough to ventilate the tachocline and to confine \mathbf{B}_i in high latitudes.

8.3 The nearly-laminar magnetic interior

Following GM98's inevitability argument we now take for granted the existence of the global-scale interior field \mathbf{B}_i , and expand our timeframe to the gigayear perspective of solar spindown. Let us accept, in particular, that the present-day interior is close to solid rotation essentially because spindown was, and presumably still is, Ferraro-constrained — in other words constrained by the Alfvénic elasticity of a sufficiently strong poloidal component of \mathbf{B}_i .

This is almost the same thing as saying that \mathbf{B}_i was, and is, strong enough to stop HSZ burrowing, allowing a helium settling layer to form. The burrowing depends on the sustained gyroscopic pumping of an MMC, whose Coriolis force accelerates a deepening layer of differential rotation in

thermal-wind balance. It is the resulting baroclinicity, together with thermal diffusion, that allows the MMC to persist and to continue burrowing. If the Ferraro constraint is strong enough to stop the differential rotation (with the help of MHD shear instabilities as necessary, see below), then it also stops the baroclinicity[†] and therefore the burrowing. In other words it impedes the response to the pumping, almost as if the interior were solid. Thus the response is limited to being an MMC such that its entire mass flux can be accepted by the thermomagnetic boundary layer at the top of the interior, as in GM98.

The estimates of Mestel & Weiss (1987) and the detailed numerical experiments of Charbonneau & MacGregor (1993, hereafter CM93) suggest that the order of magnitude required to impose the Ferraro constraint is $|\mathbf{B}_i| \gtrsim 10^{-2} \text{G}$. The GM98 inevitability argument then implies that \mathbf{B}_i must be at least this strong, in reality, and furthermore, as already mentioned, that in high latitudes \mathbf{B}_i must be largely confined to the interior by the gyroscopic pumping from above, as required in spindown scenarios like those of CM93. If the poloidal field were not so confined then its lines would diffuse upward and outward through a substantial high-latitude region, such that the Sun’s differential rotation would differ from that observed. Such scenarios are illustrated in various ways by the numerical experiments of Garaud (2002), Braithwaite & Spruit (2004), and Brun & Zahn (2006) mentioned earlier.

In spindown scenarios like those of CM93 there are poloidal-field tori within the interior, surrounding the neutral ring, that do not thread the convection zone or tachocline. In order to spin those tori down, avoiding a “dead zone” of superrotation surrounding the neutral ring and hence a contradiction with the helioseismic evidence, CM93 had to use an artificial viscosity ν far greater than the actual microscopic viscosity. In the real Sun, therefore, some kind of turbulent eddy viscosity must be involved.

Now S99 and S02 cogently argue that, when shear develops in the interior, the first turbulent process to kick in will be a small-scale dynamo mediated by Tayler instabilities — stratification-modified pinch or kink-type (‘tipping’) instabilities — of the toroidal field wound up by the shear. See also Spruit (1999), and the numerical verification of dynamo action by

[†] I use the term ‘baroclinicity’ in its most fundamental sense, meaning the nonvanishing of the $\nabla p \times \nabla \rho$ term in the three-dimensional vorticity equation, where ρ is density and p is total pressure including the hydrostatic background. In the case of thermal-wind balance this in turn implies the nonvanishing of the axial derivative of angular velocity Ω and hence, usually, violation of the Ferraro constraint. In a perfect gas the nonvanishing of $\nabla p \times \nabla \rho$ is equivalent to the nonvanishing of $\nabla p \times \nabla \vartheta$ and of $\nabla p \times \nabla T$, where T is temperature, and is therefore equivalent to having nonvanishing isobaric gradients of T .

Braithwaite & Spruit (2006). The dynamo is shear-driven and, arguably, has the robustness of an interchange instability. One may therefore reasonably assume that it will act to reduce shear through the Maxwell stresses produced by windup. In this respect it is somewhat like the better-known magnetorotational instability in hot accretion disks (e.g. Chapter 12 & refs.), which, however, has a much higher shear threshold (Spruit 1999 §4.1 & refs.). Therefore the Tayler-mediated small-scale dynamo appears likely to be the main mechanism inhibiting the formation of superrotating “dead zones” in the real Sun.

The existence of the Ferraro constraint, aided by the rapid damping of global torsional oscillations by phase mixing, implies that instability need only occur at one location on each torus. This point is significant since, unlike the magnetorotational instability, the Tayler instability tends to be ineffective near the equator and so needs the help of the Ferraro constraint, if it is to bring about uniform spindown. Without the Ferraro constraint, there would be nothing to stop global scale sub-threshold shears from building up. Near the equator, above the neutral ring, magnetorotational instability may have a role as well. Recall that by adopting sufficiently small scales the instabilities can make use of thermal diffusivity, κ , to release the constraint due to thermal stratification (e.g. Townsend 1958, Fricke 1969, Zahn 1974, Acheson 1978).

Now because spindown is so slow, we may expect the instabilities to kick in very sporadically in space and time, and certainly not uniformly throughout the interior. The Ferraro constraint is needed for that reason as well. Such sporadic or intermittent behaviour is generic for any high-Reynolds-number fluid system whose coarse-grain shear is well below all instability thresholds. In this respect the Sun’s interior must be somewhat like sheared, stably stratified terrestrial fluid systems at high Richardson number. In all such systems it is well known that turbulence occurs sporadically, the more so the higher the Richardson number. The terrestrial lower stratosphere is a case in point. The sporadic occurrence of turbulence there is familiar to everyone in these days of universal air travel. Most of the time the seat belt sign is off, and the ride almost perfectly smooth. Since coarse-grain Richardson numbers Ri are large, shear-instability thresholds $Ri \lesssim \frac{1}{4}$ cannot be exceeded over large volumes.

We are forced to conclude — because of the extreme slowness of spindown — that the Sun’s interior, even more than the terrestrial stratosphere, must be laminar at most times and locations. And, as already remarked, the whole picture is consistent with the presence of a distinct helium settling

layer in perhaps the top 100 Mm or so of the radiative envelope, for which there is some helioseismic support (Chapter 3 §5).

Corresponding estimates for the stably-stratified tachocline (S02 §5) point toward the opposite conclusion. A coarse-grain view of the tachocline puts it well above threshold, in high latitudes at least, (8.26)–(8.28) below). The high-latitude tachocline seems therefore likely to be in some sense much more turbulent than the interior. For a turbulent tachocline we need to consider how convection-zone stresses are handed over to the interior. This involves understanding how an MHD-turbulent flow goes over into a laminar, Ferraro-constrained flow. It is this problem that is considered next.

8.4 The high-latitude tachocline and its invisible shear

How then is the stress handed over? More precisely, what is the pattern of angular momentum transport, from some combination of MMCs and turbulent stresses, that transmits to each latitude of the mostly laminar, Ferraro-constrained interior any torque that arises from the convection zone’s propensity to rotate differentially? And could that pattern include an MMC capable of confining \mathbf{B}_i in a band of high latitudes — let us say something like latitudes 50° – 80° or colatitudes 10° – 40° — holding the field lines of \mathbf{B}_i nearly horizontal there against magnetic diffusion, as required to bring about Ferraro-constrained spindown in most of the interior?

Now it happens that the Tayler instability is likely to be effective in something like the same latitude band, as well as in the neighbourhood of the pole. To assess this more closely one would need to consider the latitudinal gradients of the actual toroidal field produced by the small-scale dynamo — which is why a low-latitude band might also be unstable, from time to time at least — and one would need to consider the possible shear-induced modifications of the Tayler instability itself (Chapter 10).

For the moment, however, I simply assume that there is an “active band” of high latitudes, probably something like the nominal 50° – 80° , where the vertical shear is enough to drive the Tayler-mediated small-scale dynamo and for S02’s order-of-magnitude estimates to apply. I ignore horizontal shear, in effect supposing that the tachocline is in shellular solid rotation in the active band of latitudes. The angular-velocity contours in Figure 3.7 of Chapter 3 hint that this may not be too bad an approximation.† Thus the focus is

† Shellular solid rotation in the active band is plausible, in any case, because of the shear-reducing propensities of the Tayler-mediated small-scale dynamo pointed out in S02. Indeed, unlike nonmagnetic turbulence, the small-scale dynamo could have taken on the role of the Spiegel–Zahn horizontal eddy viscosity had it not been for the dependence on the latitudinal gradients of toroidal field. That dependence precludes the small-scale dynamo from being effective across all latitude bands, implying that the GM98 inevitability argument still holds good. In order to enforce solid rotation in the manner of the Spiegel–Zahn theory, a horizontal

on the vertical structure. I further simplify by assuming a single latitudinal scale $\ell \sim 10^2$ Mm, in a formal sense staying with slab-model thinking for the moment. It will be convenient to stay with the slab-model notation as well; thus, z will still be the upward, i.e. radial, coordinate, and $\partial u/\partial z$ will be the vertical shear of the mean azimuthal velocity. (Strictly it is $\partial/\partial z$ of the mean *angular* velocity that is relevant, but the difference is unimportant for present purposes.) It will be convenient to define a nondimensional shear

$$q = \Omega^{-1} \partial u / \partial z \quad (8.17)$$

(S02's notation); the threshold value of $|q|$ will be denoted by q_{crit} . Its order of magnitude is given by (8.26) below.

The key points are listed next, followed by the order-of-magnitude relations that underpin them. It will emerge that the processes involved cover practically the entire range of timescales from gigayears down to the months and years of convective overshoot and the solar-cycle dynamo. The latter, being self-evidently a large-scale, low-latitude dynamo as well as a relatively fast one, is a different beast altogether from the small-scale, stably-stratified dynamo presently under discussion. The small-scale dynamo will turn out to be vastly slower, yet still fast in comparison with gigayears. To avoid confusion it will need to be remembered that “small-scale” refers not to horizontal scales but only to the vertical scale of the eddy motion.

- (i) The small-scale dynamo has plenty of headroom, given any of the current estimates of tachocline thickness Δ . This would be so even if the real high-latitude tachocline were as thin as the $\Delta \approx 13$ Mm $\approx 0.019R_{\odot}$ estimated by Elliott & Gough (1999), let alone the $\Delta \approx 65$ Mm $\approx 0.09R_{\odot}$ now anticipated in connection with lithium burning. The vertical scale δ_{κ} of the eddy motion, governed here by the thermal diffusivity κ acting to release the stratification constraint, is of the order of 10^{-1} Mm, Equation (8.25) below.
- (ii) The dominant azimuthal stress across horizontal area elements is the turbulent Maxwell stress. Its mean value is proportional to the local vertical shear $\partial u/\partial z$ with a proportionality coefficient ν_e , (8.24) below, that is approximately constant like an ordinary viscosity. In particular, ν_e is independent of shear for any supercritical shear $|\partial u/\partial z| > \Omega q_{\text{crit}}$. This shear-independence of ν_e is remarkable for a fully developed turbulent flow. S02 aptly calls it a “coincidence”. For the stably-stratified tachocline, $\nu_e \sim 1.6 \times 10^8 \text{ cm}^2 \text{ s}^{-1}$.

eddy viscosity would need to support a stress that transmits azimuthal torques horizontally across all latitudes. It would need to produce, respectively, prograde and retrograde torques in high and low latitudes, in just such a way as to cancel the gyroscopic pumping from above.

- (iii) So powerful is the Maxwell stress that it dominates the angular momentum transport in the bulk of the high-latitude, stably-stratified tachocline. This statement holds over a vast range of possible $|\mathbf{B}_i|$ values. It dominates even when $|\partial u/\partial z|$ is much smaller than typical coarse-grain shear values estimated from helioseismology. That is part of why the shear $|\partial u/\partial z|$ in the lower, stably-stratified portion of a 65 Mm deep ventilated tachocline may be expected to be helioseismically invisible in high latitudes. We shall see that the magnitude of ν_e is large enough to bring $|\partial u/\partial z|$ down to values close to threshold, Ωq_{crit} , in high latitudes. Such values are about an order of magnitude less than the visible shear.
- (iv) The simplest version of the implied scenario is for $|\partial u/\partial z|$ to stay just above threshold, $|\partial u/\partial z| \sim \Omega q_{\text{crit}}$. We shall see that this is possible if tachopause $|\mathbf{B}_i|$ values are large enough, $\gtrsim 10^2 \text{G}$. There are other possible scenarios, for lower $|\mathbf{B}_i|$ values, in which time-averaged $|\partial u/\partial z|$ values are sub-threshold and the dynamo action intermittent. In such cases ν_e takes $|\partial u/\partial z|$ below threshold and switches off, $|\partial u/\partial z|$ then builds up through gyroscopic pumping (temporarily like an unsteady version of the GM98 scenario), then ν_e switches on again, and so on cyclically. Possible cycle times could be anywhere in the range from $\sim 10^6 \text{y}$ upward, depending on $|\mathbf{B}_i|$.
- (v) In the bulk of the stably-stratified tachocline, thermal-wind balance holds robustly. There, the weak vertical shear constrains baroclinicity *qua* latitudinal buoyancy gradients $|\partial \vartheta/\partial y|$ to be weak as well. Furthermore, the dynamo turbulence leaves unaffected both the N value of the subadiabatic thermal stratification itself and the value of κ felt by mean motions (H. Spruit, personal communication). This is because of the way the turbulent motion depends on κ to release the stratification constraint. So MMCs are still tied to $|\partial \vartheta/\partial y|$ via the microscopic κ value, $\sim 10^7 \text{cm}^2 \text{s}^{-1}$, just as if the turbulence were absent, i.e. in just the same way as in GM98. The upshot is that in the bulk of the stably-stratified tachocline there is no MMC, to a first approximation, and that even with the weakened $|\partial u/\partial z|$ the angular momentum transport, there, is mediated predominantly by ν_e . To a higher approximation, one might expect an MMC like GM98's except that there is now no impediment to weak equatorial downwelling.
- (vi) One peculiar consequence is that in stark contrast with GM98 the present scenario, as developed so far, appears to leave Δ values almost completely unconstrained. This opens the possibility already mentioned that Δ is large enough, $\approx 65 \text{Mm}$, to explain lithium burning,

even with no “polar pits”. It seems that Δ is determined in a rather subtle and delicate way, not amenable to simple order-of-magnitude analysis. Indeed it may well be that Δ is not determined by quasi-steady dynamics but, rather, depends on the history of convection-zone retreat and helium settling layer formation, as well as on $|\mathbf{B}_i|$ values. (Thus the scatter in lithium abundance found in samples of solar-type stars might be related to a scatter in $|\mathbf{B}_i|$ values as well as to rotation histories.)

- (vii) The dynamo begins to lose headroom in a lowermost turbulent layer of thickness $\sim \delta_\kappa \sim 10^{-1}$ Mm. Notice from (8.25) that the scale δ_κ is, like ν_e , independent of shear, as long as the dynamo is switched on. As we enter the lowermost turbulent layer, vertical eddy scales and ν_e values must decrease downward. Shear values $|\partial u/\partial z|$ increase, but not enough to stop the turbulent Maxwell stress from diverging and giving rise to an azimuthal force \bar{F} , hence gyroscopic pumping.
- (viii) A slight extension of S02’s arguments suggests that $\nu_e \propto z^2$ within the lowermost turbulent layer, joining continuously to the constant value $\nu_e \sim 1.6 \times 10^8 \text{ cm}^2 \text{ s}^{-1}$ in the bulk of the tachocline, where z is measured from some virtual origin near the bottom of the lowermost layer. Further analysis suggests that the azimuthal and meridional turbulent Maxwell stress components

$$\nu_e \left(\frac{\partial u}{\partial z}, \frac{\partial v}{\partial z} \right) = (\sigma, \tau), \quad (8.18)$$

say, take on a modified Ekman-layer structure, breaking the thermal-wind constraint as well as gyroscopically pumping an MMC in the form of a poleward Ekman mass flux. Note that this pumping is entirely due to the fluctuating Maxwell stresses described by the eddy viscosity ν_e , and nothing whatever to do with the sort of quasi-steady Maxwell stresses that would characterize a laminar Hartmann or Ekman–Hartmann layer, or the thermomagnetic boundary layer of GM98.

- (ix) To the extent that we have shellular solid rotation $\Omega(z)$ in the active band of latitudes, and the dynamo is switched on, the poleward Ekman mass flux must converge so as to produce an approximately uniform downwelling, $w_{\text{Ek}} < 0$. To see this one has to depart from slab-model geometry and substitute spherical or polar cylindrical geometry. The vertically integrated mass-flux convergence is approximately uniform for the same reasons as in ordinary laminar spindown in a laboratory cylinder. It is only the vertical structure, not the ver-

tically integrated mass flux, that is changed by the vertically variable eddy viscosity within the modified Ekman layer. Indeed we have the simple formula

$$w_{\text{Ek}} = \nu_e \left. \frac{d(\ln \Omega)}{dz} \right|_{\text{bulk}}, \quad (8.19)$$

implying $w_{\text{Ek}} < 0$ since $d(\ln \Omega)/dz|_{\text{bulk}} < 0$ in the high-latitude tachocline. The value of ν_e in (8.19) is just the constant bulk value $\nu_e \sim 1.6 \times 10^8 \text{ cm}^2 \text{ s}^{-1}$ outside the layer. The formula is readily derived by assuming incompressible flow together with the gyroscopic-pumping relation (8.3), setting $\bar{F} = \partial \sigma / \partial z$ in (8.3), then integrating across the modified Ekman layer and computing the horizontal volume-flux convergence in polar geometry. So (8.19) depends only on the fact that $\sigma(z)$ drops from $\nu_e \partial u / \partial z|_{\text{bulk}}$ down to zero across the modified Ekman layer, as the small-scale dynamo finally runs out of headroom. It does not depend at all on the detailed vertical structure within the modified Ekman layer.

- (x) The downwelling described by (8.19) is prevented by \mathbf{B}_i from burrowing into the interior, as noted in §8.3. Having nowhere else to go, the mass flux must recirculate through a laminar thermomagnetic boundary layer of thickness $\delta_{\kappa\eta}$, say, like that proposed in GM98, lying immediately beneath the modified Ekman layer and forming with it a tight double-boundary-layer structure. Values of $\delta_{\kappa\eta}$, (8.30) below, go like $|\mathbf{B}_i|^{-1/3}$ but are typically a fraction of a megametre. Thus we have convergent poleward flow in the lowermost turbulent layer, and divergent equatorward flow in the laminar thermomagnetic boundary layer just beneath. It is in this way that the stress transmitted by ν_e , i.e. by the averaged *fluctuating* Maxwell stress in the bulk of the stably-stratified tachocline, is handed over via the MMC in the lowermost tachocline to the *quasi-steady* Maxwell stress in the outermost fringe of the laminar interior — which fringe is just the thermomagnetic boundary layer. That boundary layer therefore has a dual role: it serves both as the laminar sublayer of the turbulent lowermost tachocline, and also as the outermost fringe of the laminar, Ferraro-constrained interior. It is here that the Ferraro constraint begins to make itself felt directly, through the downwelling and advective-diffusive balance in the boundary layer as discussed in GM98. And it is this same downwelling and advective-diffusive balance that brings about the high-latitude confinement of \mathbf{B}_i , in the same way as in GM98.

The order-of-magnitude relations on which the foregoing statements are based are now summarized. The relations are equivalent to those in S02 except that I revert to formal slab-model thinking and use $\ell \sim 10^2$ Mm as the latitudinal scale instead of the tachocline radius r used in S02; the scale ℓ roughly corresponds to what GM98 called r/L . As in S02 I also ignore factors like $2 \cos \theta$ in front of Ω , where θ is colatitude, and factors like π .

The formal assumption of a single latitudinal scale ℓ may not be as bad as it sounds, despite the importance of the real polar geometry for the pattern of mass transport in the MMC, as noted in point (ix) above. The Tayler instability, as such, has a large horizontal reach because of its kink or tipping-type kinematics dominated by azimuthal wavenumber $m = 1$. It is certainly able to reach across the pole — one might say more aptly “slide across the pole”, as suggested in Figure 1 of S99 — and will probably do so even though the mean shear defined by azimuthal averaging must, technically speaking, vanish at the pole. The instability is a physical process with no respect for coordinate singularities. Indeed, it tends to use as much horizontal space as is available to it, and S02’s estimates assume that it does so. As in GM98, the scale ℓ is meant to be no more than a rough way of characterizing the magnitudes of horizontal derivatives constrained by the available horizontal space.

Let η be the microscopic magnetic (ohmic) diffusivity and Ω_A the typical toroidal field strength produced by the small-scale dynamo within the tachocline, measured as angular Alfvén speed, i.e. as the number of radians of longitude per unit time travelled by the phase of an Alfvén wave. We assume that the microscopic diffusivities satisfy

$$\kappa \gg \eta \gg \nu, \quad (8.20)$$

consistent with typical numerical orders of magnitude $\kappa \sim 1.4 \times 10^7 \text{ cm}^2\text{s}^{-1}$, $\eta \sim 4 \times 10^2 \text{ cm}^2\text{s}^{-1}$, $\nu \sim 3 \times 10^1 \text{ cm}^2\text{s}^{-1}$ near the top of the tachocline, at $0.7R_\odot$ and $\kappa \sim 1 \times 10^7 \text{ cm}^2\text{s}^{-1}$ and $\eta \sim 3 \times 10^2 \text{ cm}^2\text{s}^{-1}$ at $0.62R_\odot$ (Chapter 1, Table 1.1ff.). Following S99 and S02 we assume

$$N \gg \Omega \gg \Omega_A, \quad (8.21)$$

the first of which is well satisfied with thermal buoyancy frequency $N \sim 10^{-3} \text{ s}^{-1}$, and $\Omega \sim 3 \times 10^{-6} \text{ s}^{-1}$. The second is also well satisfied because, defining the dimensionless thermal diffusivity and Prandtl–Rossby ratio by

$$K = \kappa/N\ell^2 \sim 10^{-10}, \quad P = \Omega/N \sim 3 \times 10^{-3}, \quad (8.22)$$

with $\kappa = 1 \times 10^7 \text{ cm}^2\text{s}^{-1}$ and $\ell = 10^2 \text{ Mm} = 10^{10} \text{ cm}$, we have from S02

equation (19)[†] that

$$\Omega_A/\Omega = q^{1/2}(KP)^{1/8} \ll 1, \quad (8.23)$$

since the dimensionless shear $q \lesssim 1$ even with extreme assumptions, as will emerge shortly. Now a slight rearrangement of equations (10) and (32) of S02 produces[†]

$$\nu_e = \ell^2 \Omega (KP)^{1/2} = \Omega \delta_\kappa^2 \sim 1.6 \times 10^8 \text{ cm}^2 \text{ s}^{-1}; \quad (8.24)$$

where

$$\delta_\kappa = \ell (KP)^{1/4} \sim 0.7 \times 10^{-1} \text{ Mm}. \quad (8.25)$$

The second formula for ν_e in (8.24) shows at once why the lowermost turbulent layer of thickness $\sim \delta_\kappa$ will have the characteristics of an Ekman layer, point (vii) above, since not only is δ_κ independent of q , the “coincidence” mentioned in point (ii) above, but also, by a further coincidence, δ_κ is the same as the Ekman thickness scale $(\nu_e/\Omega)^{1/2}$.

The dimensionless shear threshold or critical shear for the small-scale dynamo to operate is, from S02 (27),

$$q_{\text{crit}} = K^{1/4} P^{-7/4} (\eta/\kappa) \sim 2.5 \times 10^{-3} \quad (8.26)$$

at $0.62R_\odot$. Reading Ω values from the horizontal contours in Figure 3.7 of Chapter 3, we see that Ω goes from about 390 to 430 nHz, corresponding to a fractional change

$$\alpha = (430 - 390)/410 = 1 \times 10^{-1} \quad (8.27)$$

from which we may derive a nominal q value, with the conservative choice $\Delta = 65 \text{ Mm}$,

$$q = \alpha \ell / \Delta \sim 1.5 \times 10^{-1}. \quad (8.28)$$

Even with such a large Δ this nominal shear is nearly two orders of magnitude greater than q_{crit} . However, as already noted, the stress and therefore

[†] As long as the small-scale dynamo’s toroidal magnetic field is expressed as the Alfvén angular velocity Ω_A , the spherical and cylindrical radii, as such, do not enter any of the formulae being quoted from S02. The significance of the symbol r in S02 is always that of the available latitudinal lengthscale. That is why the formulae are written here using ℓ in place of r .

[†] All these expressions depend on S99 Equation (49) after correcting a typographic error: the last occurrence of N should be Ω ; see Equation (A29) of S99 and footnote on p 927 of S02. We may note also that the statement on S99 page 194b that “rotation does not by itself remove the instability” is made in the wrong context, that of zero diffusivities. The statement is correct for the real-world *diffusive* problems of interest here, but incorrect for a diffusionless problem. This latter point is illustrated by Equation (10.15) in Chapter 10, which is for the kink or tipping mode, azimuthal wavenumber $m = 1$, of a diffusionless Tayler instability in the case of solid background kinetic rotation Ω and Alfvénic rotation Ω_A . In that diffusionless case, $\Omega \geq \Omega_A$ implies stability.

the actual shear, in the bulk of the stably-stratified tachocline, is tightly linked by (8.19) to the downwelling velocity w_{Ek} , which must equal the downwelling velocity $w_{\kappa\eta}$ that can be accepted by the thermomagnetic boundary layer. That is why the actual shear, in the stably-stratified tachocline, is likely to be far smaller than the nominal shear just computed — though still dynamically significant, sharply distinguishing the tachocline from the interior — and why a tachocline 65 Mm deep could be consistent with the high-latitude Ω contours in Figure 3.7 of Chapter 3, despite appearances.

We assume that GM98's estimate of $w_{\kappa\eta}$ is correct in order of magnitude:

$$|w_{\kappa\eta}| \sim \eta/\delta_{\kappa\eta} \propto |\mathbf{B}_i|^{1/3} \propto V_{\text{Ai}}^{1/3}, \quad (8.29)$$

where V_{Ai} is the interior Alfvén speed corresponding to $|\mathbf{B}_i|$, about 0.4 cm s^{-1} per gauss near $0.62R_\odot$, with density $\rho \sim 0.42 \text{ g cm}^{-3}$, and where the boundary-layer thickness scale is

$$\delta_{\kappa\eta} = K^{1/3} \left(\frac{\eta}{\kappa}\right)^{1/6} \left(\frac{\Omega\ell}{V_{\text{Ai}}}\right)^{1/3} \ell, \quad \propto (\kappa\eta)^{1/6}. \quad (8.30)$$

Equating w_{Ek} to $w_{\kappa\eta}$ and using (8.17) and (8.19), with $\partial u/\partial z \sim \ell \partial\Omega/\partial z$, we have

$$q \sim \ell \left. \frac{d(\ln \Omega)}{dz} \right|_{\text{bulk}} = \ell \frac{w_{\text{Ek}}}{\nu_e} \sim K^{-1/3} \left(\frac{\eta}{\nu_e}\right) \left(\frac{\kappa}{\eta}\right)^{1/6} \left(\frac{V_{\text{Ai}}}{\Omega\ell}\right)^{1/3}, \quad (8.31)$$

equivalently

$$V_{\text{Ai}} \sim \Omega \ell q^3 K \left(\frac{\nu_e}{\eta}\right)^3 \left(\frac{\eta}{\kappa}\right)^{1/2}. \quad (8.32)$$

For an extreme value $|q| \sim 1$ this would imply an impossibly large $|\mathbf{B}_i|$ of the order of thousands of megagauss, again suggesting that $|q| \ll 1$ and further supporting our earlier assumption (8.23). It should be cautioned, however, that GM98's scaling relation (8.29) has yet to be verified by a full analysis of the boundary-layer structure, and indeed $\delta_{\kappa\eta}$ and therefore (8.31)–(8.32) might well change at high $|\mathbf{B}_i|$ values, because Maxwell stresses then modify the meridional momentum balance assumed in GM98 (P. Garaud in Chapter 7). For $|q| = q_{\text{crit}}$ we have a more reasonable value $V_{\text{Ai}} = V_{\text{Ai}(\text{crit})}$, say, corresponding to $|\mathbf{B}_i| \sim 10^2 \text{ G}$. This follows from (8.24), (8.26) and (8.32):

$$\begin{aligned} V_{\text{Ai}(\text{crit})} &= \Omega^4 \ell^7 K^{13/4} P^{-15/4} \eta^{1/2} \kappa^{-7/2} \\ &= \Omega \ell K^{1/4} P^{-3/4} (\eta/\kappa)^{1/2} \sim 0.4 \times 10^2 \text{ cm s}^{-1}, \end{aligned} \quad (8.33)$$

implying in turn that $\delta_{\kappa\eta} \sim 0.7 \times 10^{-1} \text{ Mm}$ and that $w_{\kappa\eta} = w_{\text{Ek}} \sim 4 \times 10^{-5} \text{ cm s}^{-1}$. This magnitude $V_{\text{Ai}(\text{crit})} \sim 0.4 \times 10^2 \text{ cm s}^{-1}$ or $|\mathbf{B}_i| \sim 10^2 \text{ G}$

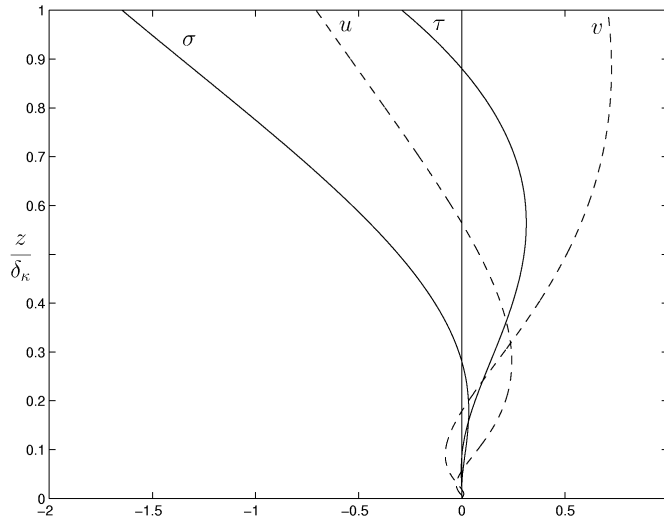


Fig. 8.1. Solutions of (8.18), (8.34) regarded as an idealized model of the lower portion of the modified Ekman layer where the eddy viscosity $\propto z^2$. Somewhat arbitrarily, this lower portion is assumed to occupy a layer of thickness δ_κ , in dimensionless coordinates $0 \leq z \leq 1$. Again somewhat arbitrarily, the eddy viscosity in (8.18) is taken to have reached the value $\frac{1}{2}\nu_{e\infty}$ at $z = 1$, i.e. half the asymptotic value $\nu_{e\infty} \sim 1.6 \times 10^8 \text{ cm}^2\text{s}^{-1}$ in the bulk of the stably-stratified tachocline above. The solutions finite at $z = 0$ are then $(u, v) = (\text{Re}, \text{Im}) e^{3i\pi/4} z^a$ and $(\sigma, \tau) = z^2 \partial(u, v)/\partial z = (\text{Re}, \text{Im}) a e^{3i\pi/4} z^{a+1}$, in dimensionless units, where $a = \frac{1}{2}\{-1 + \sqrt{(1 + 16i)}\} = 0.9591 + 1.3707i$. In fact there is a 1-parameter family of solutions with $a = \frac{1}{2}\{-1 + \sqrt{(1 + 4iC)}\}$, where $C = 4z_{1/2}^2$ with $z_{1/2}$ the dimensionless altitude at which the eddy viscosity reaches the value $\frac{1}{2}\nu_{e\infty}$. Such solutions cannot describe the upper portion of the layer where the viscosity profile approaches its asymptotic value $\nu_{e\infty}$, nor can they correctly describe the fine details near the bottom of the real modified Ekman layer where it interfaces with the thermomagnetic boundary layer. This is because the dynamo runs out of headroom somewhere *above* $z = 0$, depending on $|\mathbf{B}_i|$ values. The saving grace, however, is that the mass-flux relation (8.19) depends only on σ going to zero somehow, and not on the detailed vertical structure.

represents the critical order of magnitude of \mathbf{B}_i above which the stably stratified, high-latitude tachocline can continuously sustain small-scale dynamo action and below which the dynamo action would have to be intermittent, point (iv) above.

A curious aspect of the scaling (8.33) is the implication that $V_{\text{Ai}(\text{crit})} = \ell \Omega_A$ at threshold. One may see this by substituting (8.26) into (8.23). Therefore the critical magnitude of \mathbf{B}_i — whose most important component for this purpose is the *poloidal* component, as explained in GM98 —

coincides with the order of magnitude of the Tayler-unstable eddy *toroidal* field of the small-scale dynamo. Furthermore, we see from (8.30) and (8.33) that $V_{\text{Ai}} = V_{\text{Ai(crit)}}$ implies $\delta_{\kappa\eta} \sim \delta_{\kappa}$. It seems that, just above threshold, the scaling for the small-scale dynamo eddies is the same as GM98's scaling for the thermomagnetic boundary layer. This is perhaps not unreasonable since both structures have shallow aspect ratios δ_{κ}/ℓ , $\delta_{\kappa\eta}/\ell$ and both, at threshold, feel not only a strong Coriolis effect but also the magnetic as well as the thermal diffusivity. We may also note from S02 (3) that, under these threshold conditions, the eddy timescale for the small-scale dynamo, i.e. the growth time for the Tayler instability, is $\Omega/\Omega_A^2 \sim 10^4 \text{y}$ — fast from some viewpoints and slow from others.

A full analysis of the double-boundary-layer structure is beyond our scope here, and awaits further investigation. However, in the lower portion of the modified Ekman layer, where we are provisionally supposing that the eddy viscosity falls off like z^2 as the small-scale dynamo runs out of headroom, points (vii) and (viii) above, the Ekman-layer equations have complex power-law solutions that give some idea of the structure. Figure 8.1 shows some possible profiles of σ , u , τ and v . These satisfy (8.18) with $\nu_e \propto z^2$ together with the standard Ekman-layer equations

$$-2\Omega v = \partial\sigma/\partial z, \quad 2\Omega u = \partial\tau/\partial z; \quad (8.34)$$

see caption for further details. The profiles give what seems to be a qualitatively reasonable description of the lower portion of the modified Ekman layer, showing how the shears can stay finite and the stresses go to zero as $z \rightarrow 0$. There is another set of complex power-law solutions, rejected as unphysical, for which the shears and stresses go to infinity as $z \rightarrow 0$.

In the upper portion of the layer, not shown, where the power-law solutions cease to apply, as the eddy-viscosity profile departs from its z^2 dependence and begins to approach its asymptotic value $\nu_{e\infty} \sim 1.6 \times 10^8 \text{cm}^2 \text{s}^{-1}$ in the bulk of the stably-stratified tachocline above, we can imagine the profiles being smoothly continued upward with τ and v making an oscillatory approach to zero in the usual manner of Ekman profiles. The azimuthal stress σ must continue toward its asymptotic negative value $\nu_{e\infty} \partial u/\partial z|_{\text{bulk}}$, and the azimuthal shear $\partial u/\partial z$ toward a corresponding negative value, smaller in magnitude than in the portion of the u profile visible in Figure 8.1, point (vii) above. Again one expects an oscillatory approach toward these asymptotes. A consistent description of the upward continuation requires the second of (8.34) to be replaced by an equation corresponding to a steady, variable-viscosity version of (8.2c) with a small but significant thermal-wind term, as already hinted by the scaling relation $\delta_{\kappa\eta} \sim \delta_{\kappa}$. That is a further sense

in which the Ekman layer is ‘modified’. The v profile and its upward continuation describe, of course, the gyroscopically-pumped poleward flow.

The issue of tachocline ventilation turns out to involve subtleties that depend on the effects of compositional stratification N_μ . So we discuss the latter first.

8.5 The effects of compositional stratification N_μ

As already emphasized, the helium settling layer just beneath the tachocline owes its existence to the suppression of global-scale HSZ burrowing by the interior field \mathbf{B}_i . Once the settling layer has formed, the vertical gradient of mean molecular weight μ adds a contribution

$$N_\mu^2 = -g \partial \ln \mu / \partial z \quad (8.35)$$

to the buoyancy frequency squared that is a significant fraction of the typical thermal value $N^2 \sim 10^{-6} \text{ s}^{-2}$. For instance, a standard solar model (Figure 3.4 of Chapter 3) gives a fractional contrast $d \ln \mu = 0.014$ across the settling layer and a corresponding reduced gravity $g' = 0.014g \sim 0.9 \times 10^3 \text{ cm s}^{-2}$. Measuring the slope shown in the inset to Figure 3.4a, one gets $\partial/\partial z \sim (0.05R_\odot)^{-1} \sim (35 \text{ Mm})^{-1}$; so $N_\mu^2 \sim g'/0.05R_\odot \sim 0.25 \times 10^{-6} \text{ s}^{-2}$, or $N_\mu \sim 0.5 \times 10^{-3} \text{ s}^{-1}$. However, neither $d \ln \mu$ nor N_μ^2 can really be said to be known precisely, because as discussed in Chapter 3 the helioseismic evidence is undergoing revision, though still generally supporting the existence of the settling layer. It is possible that the real settling layer may be somewhat deepened, with $\partial/\partial z$ perhaps more like $(100 \text{ Mm})^{-1}$, by the weak and highly sporadic interior turbulent mixing discussed in §8.3. Furthermore, the overall μ contrast across the layer could be somewhat bigger than indicated by the number $d \ln \mu = 0.014$, if the same weak mixing were even slightly effective in bringing up helium-rich gas from the core, on the gigayear timescale. Fortunately, however, the following arguments depend only on very rough orders of magnitude for $d \ln \mu$ and N_μ^2 .

The main issue is whether HSZ burrowing can penetrate the interior near the polar weak spots in \mathbf{B}_i , as speculated in GM98. These are the zero points or “hairy-sphere defects” of the vector field formed by the horizontal projection of \mathbf{B}_i . If such burrowing were possible, then it could create “polar pits” or “cauldrons”, in which lithium could be burned even if Δ were less than 65 Mm. The most favourable conditions for such burrowing would be that $|\mathbf{B}_i|$ is altogether negligible near the poles. We ask whether, in that most favourable case, the burrowing could locally penetrate the helium settling layer in those neighbourhoods. It will appear that the answer is a clear “no”.

The nonmagnetic slab model of §8.2 is sufficient to reveal the essential effects, which turn out to be insensitive to the choice of horizontal scale ℓ . The only changes needed are to replace the thermal buoyancy acceleration ϑ by the total buoyancy acceleration $\vartheta + \vartheta_\mu$ in (8.2c), and to append an equation for the compositional buoyancy acceleration ϑ_μ . In the latter equation we may safely neglect all diffusive effects, which are tiny.† By analogy with the thermal buoyancy acceleration we define ϑ_μ as g times the fractional departure of μ from its background stratification, so that the equation for ϑ_μ is

$$\frac{\partial \vartheta_\mu}{\partial t} + N_\mu^2 w = 0, \quad (8.36)$$

in which we idealize by taking $N_\mu = \text{constant}$. Simplifying (8.2c) as before, we have the appropriate form of the thermal-wind equation,

$$2\Omega \frac{\partial u}{\partial z} + \frac{\partial(\vartheta + \vartheta_\mu)}{\partial y} = 0, \quad (8.37)$$

and readily find that (8.15) is replaced by

$$\left\{ \left(\frac{\partial}{\partial t} - \kappa_\mu \frac{\partial^2}{\partial z^2} \right) \frac{\partial^2}{\partial y^2} - \frac{4\Omega^2 \kappa}{N^2} \frac{\partial^4}{\partial z^4} \right\} \frac{\partial u}{\partial t} = \left(\frac{\partial}{\partial t} - \kappa_\mu \frac{\partial^2}{\partial z^2} \right) \frac{\partial^2 \bar{F}}{\partial y^2} \quad (8.38)$$

where $\kappa_\mu = \kappa N_\mu^2 / N^2$. The microscopic viscosity ν has been neglected, since it is nearly as small as the helium self-diffusivity, $\chi \sim 10^1 \text{ cm}^2 \text{ s}^{-1}$, which has already been neglected in (8.36).

Now the key point is that (8.38) is an equation for $\partial u / \partial t$ and not for u . The $\partial / \partial t$ is a crucial and essential feature, coming from the need to eliminate ϑ_μ between (8.36) and (8.37). By contrast, ϑ is eliminated as in the derivation of (8.15), via (8.2d) with its $\partial / \partial t$ neglected. That is appropriate because of the enormous magnitude of $\kappa \sim 10^7 \text{ cm}^2 \text{ s}^{-1}$ relative to χ .

With a relatively small horizontal scale ℓ — as before, we consider slab-model solutions sinusoidal in y/ℓ — one might think at first that the new quasi-diffusive term in κ_μ signals the possibility of burrowing straight down into the helium settling layer. But appearances are deceptive here.

Consider a thought-experiment in which the forcing is switched on at time zero. The time-dependent solutions of (8.38) below the forcing layer, right-hand side zero, describe burrowing that commences in just the same way as with the Spiegel–Zahn equation (8.15). The hyperdiffusive term dominates the new quasi-diffusive term in the earliest stages, in which the vertical scale increases from zero. As the disturbance penetrates more deeply, however, the quasi-diffusive term comes into balance with the hyperdiffusive term.

† For instance $\chi \sim 10^1 \text{ cm}^2 \text{ s}^{-1}$, where χ is the self-diffusivity of helium anomalies in the appropriate hydrogen–helium mixture (Chapter 1, Table 1.1).

Thus $\partial u/\partial t$ reaches a steady state with vertical structure $\exp(z/h)$ where the vertical scale h is given by $h = (2\Omega\ell/N)(\kappa/\kappa_\mu)^{1/2} = 2\Omega\ell/N_\mu$. This is just the (nondiffusive) Rossby height belonging to the horizontal scale ℓ , and the response, from then onward, is nothing but the well-known Eliassen response to gyroscopic pumping in a nondiffusive stratified fluid. Its most important feature, for our purposes, is that $\partial u/\partial t$ and $\partial\vartheta_\mu/\partial t$ are steady, not u and ϑ_μ . The other variables ϑ , v and w are all steady. The response consists of perpetual spindown, with u and ϑ_μ asymptotically proportional to t .

This means, of course, that the response is self-limiting, in one of two possible ways. The first way is for the spindown to continue — with the u and ϑ_μ terms in (8.37) asymptotically proportional to t — until the compositional stratification surfaces are overturned and the stratification is wiped out. That is what would have taken place on a global scale, preventing the helium settling layer from forming at all, had there been no \mathbf{B}_i and no Ferraro constraint. Such a response is a nonlinear response, outside the scope of our linearized equations.

The second way, which is the one relevant here, is well within the scope of the equations. If, as here, the gyroscopic pumping is ultimately due to the convection zone's propensity to rotate differentially, then there is a saturation value beyond which the spindown cannot proceed, having taken up all the available differential rotation and thus killed off the gyroscopic pumping. We may say that the underlying layers are fully spun down. Just what the final saturation value might be is difficult to say, but one may reasonably suppose that spindown cannot proceed beyond limits governed by the value of α in (8.27), $\alpha \sim 10^{-1}$, the fractional angular-velocity increment across the whole tachocline. It is easy to verify (see the Margules-slope estimate below) that such limits are essentially zero for present purposes. They tell us that the self-limiting of the Eliassen response would take place with hardly any tilting of the compositional isopleths.

In other words, for realistic α the helium settling layer spanning the poles presents an almost perfect barrier against HSZ burrowing. That is why the polar pits cannot be dug.

Two further points need comment. The first is that (8.38) also admits perpetual-spindown solutions with a linear dependence on z , such as $u \propto t \sin(y/\ell)$ and $w \propto zt \sin(y/\ell)$. These, however, fail to satisfy physically reasonable boundary conditions. For instance the first of them requires both $|\vartheta|$ and $|\kappa\partial\vartheta/\partial z|$ to increase like t at the top boundary, if $w = 0$ at some bottom boundary. This is because ϑ has to be asymptotically proportional to $zt \cos(y/\ell)$ in order to avoid violating (8.37), in which $\partial u/\partial z = 0$ despite

the perpetual tilting of μ -surfaces, implying $\vartheta = -\vartheta_\mu$. The second solution has a similar pathology and, furthermore, does not even permit $w = 0$ at the bottom, since it can be shown to imply a z -independent contribution to w , $\propto t \cos(y/\ell)$. Also, both types of solution would disappear if any horizontal heat diffusion were allowed. So we need not consider them further.

The second point is that the tilting of compositional isopleths or stratification surfaces is so small, in fact, that it tightly constrains vertical displacements of the tachopause even on a global scale. We have just found that HSZ burrowing is ineffective even at the polar weak spots of \mathbf{B}_i . Still less is it effective in the rest of the interior where the Ferraro constraint has control. There is no MMC to tilt the thermal, or overturn the compositional, stratification surfaces. The implication is that those surfaces must be accurately horizontal, in the sense that they accurately follow the gravitational–centrifugal helipotentials.

As a check on that assertion, and to get some idea of its error bar, let us calculate the tilting of compositional stratification surfaces that would occur if they alone were tilted and if the Ferraro constraint were artificially relaxed, to permit a thermal-wind shear across the helium settling layer of the same order as the shear across the whole of the high-latitude tachocline. The slope can be obtained from the thermal wind equation (8.37) evaluated with ϑ_μ alone, or equivalently and more directly from the Margules slope formula $2\Omega U/g'$ where $U \sim \Omega\alpha\ell$, the velocity increment across the layer, and α the fractional angular-velocity increment as before. Even with the extreme value $\alpha \sim 10^{-1}$ we have $U \sim 3 \times 10^3 \text{ cm s}^{-1}$ and a Margules slope $2\Omega^2\alpha\ell/g' \sim 2 \times 10^{-5}$. The nominal elevation change over a distance $r \sim 500 \text{ Mm}$ is only 10^{-2} Mm . The real elevation change from pole to equator, with the Ferraro constraint brought back into play, is therefore far, far smaller still — a very tiny fraction of a megametre indeed.

8.6 Concluding remarks

The main issue not yet addressed is that of the tachocline’s ventilation timescale. This turns out to be by far the most delicate issue, and crude order-of-magnitude arguments are unable to decide it directly. Taken at face value, the threshold numbers used in §8.4 imply gigayear ventilation times. This is because the main ventilation mechanism is now turbulent mixing by the small-scale dynamo. From S02 (15), (19), or first of (43), we have an eddy diffusivity D for vertical material transport of the order of

$$D \sim q\Omega\ell^2 P^{3/4} K^{3/4}, \quad (8.39)$$

in the notation of §8.4. If q is close to its threshold, q_{crit} , then one may verify by substitution from (8.26) that D is of the same order as the microscopic magnetic diffusivity $\eta \sim 300\text{--}400 \text{ cm}^2\text{s}^{-1}$. With $\Delta \sim 65 \text{ Mm}$ the nominal ventilation time Δ^2/η is then about the same as the Sun's main-sequence lifetime, $\sim 4 \text{ Gy}$. Perhaps this is not an accident: could it be that the thickness of the tachocline is such that it can only just stay ventilated?

One can imagine playing games with factors like π^2 or taking one or two tens of megametres off the Δ value by assuming a deep overshoot layer, or one could suppose that the small-scale dynamo in the stably-stratified tachocline is well above threshold, with the implication from (8.32) that $|\mathbf{B}_i| \gg 10^2 \text{ G}$. And when a full analysis of the double-boundary-layer structure becomes available, including a quantitative numerical model, then the net effect of the numerical factors might go one way or the other. As regards large $|\mathbf{B}_i|$, there seems no reason why the Sun should not have an interior field as strong as that of ordinary (non-neutron) magnetic stars, which should allow us to consider $|\mathbf{B}_i|$ values perhaps into the hundreds of kilogauss, magnetic escapology permitting. If, despite the cautionary remark below (8.32), the 1/3 power in (8.31) were to apply over the whole range of $|\mathbf{B}_i|$ and $|V_{\text{Ai}}|$ values, then we would be able to use $D \sim 10\eta$.

However, we may also invoke Occam's razor, appealing to the effects of compositional stratification discussed in §8.5. The key point is again the dynamical impossibility of significantly tilting the compositional isopleths in the helium settling layer. This presents a powerful barrier not only against the burrowing of MMCs but also against the turbulent erosion of heavy elements *into* the tachocline. Erosion rates must be severely limited by that circumstance alone. They will be further limited by the diffusive leakage of \mathbf{B}_i across the tachopause, and into the tachocline, in those latitude bands equatorward of the active high-latitude band where there is either no confining downwelling, or very weak downwelling such as might occur over the equator (point (v) on page 18). In such latitude bands the Ferraro constraint will reach across the tachopause, now defined as the top of the helium settling layer, and will tend to suppress shear across it and protect it from any kind of erosion. So the tachocline could be helium-poor, therefore, not so much because of fast ventilation from above, as in the GM98 scenario, but because of minuscule erosion rates of heavy elements across such a heavily-protected compositional tachopause.

There remains, however, the lithium problem, which of itself still argues for substantial ventilation. But further discussion must await detailed solutions of the nonlinear equations for the double-boundary-layer structure, as well as a more quantitative description of the small-scale dynamo.

One final twist in the tail of this tale. The *visible* shear at the top of the high-latitude tachocline — visible, for instance, in Figure 3.7 of Chapter 3 and already indicated by helioseismology to occupy mainly the lower convection zone and its overshoot layer (Chapters 1, 3 & refs.) — would be dynamically impossible in the presence of the small-scale dynamo. That is very clear from Spruit’s order-of-magnitude relations as used in §8.4, to the extent that (8.29) correctly indicates the thermomagnetic boundary layer’s mass-carrying capability. At first sight it might seem paradoxical: “surely the lower convection zone and overshoot layer is much more turbulent?” But that would be to underestimate the power of the Maxwell stresses in the small *vertical* scale dynamo, arising from the large *horizontal* reach of its eddy structures via the Tayler instability’s kink or tipping-type kinematics, dominated by azimuthal wavenumber $m = 1$, and reflected in the large vertical eddy viscosity ν_e . So the suggestion must be that the convective plumes break up that horizontal structure, disconnecting and reconnecting the wound-up field lines in such a way as to drastically reduce the eddy viscosity and permit much larger shears.

Acknowledgements. I thank the organizers, in alphabetical order Pascale Garaud, Douglas Gough, David Hughes, Bob Rosner, Nigel Weiss, and Jean-Paul Zahn, for inviting me to participate in this interesting and stimulating Workshop. Joergen Christensen-Dalsgaard kindly tutored me on everything about solar models and their notational conventions, Pascale Garaud stimulated me to reexamine the GM98 thermomagnetic boundary layer scaling, leading to the cautionary remarks about large $|\mathbf{B}_i|$, Nigel Weiss patiently helped me to improve my general knowledge of MHD and other astrophysical processes, and at the eleventh hour Douglas Gough kindly shared with me his careful calculations of diffusivity values as well as offering wise and helpful comments on many aspects of the problem. Above all, however, on this occasion, I am grateful to Henk Spruit for an extensive correspondence that helped me to improve my understanding of the Tayler-mediated small-scale dynamo and of magnetic stability, instability, and escapology.

References

- Acheson, D. J., 1978: On the instability of toroidal magnetic fields and differential rotation in stars. *Phil. Trans. Roy. Soc. Lond.*, **289**, 459–500.
- Braithwaite, J. & Spruit, H. C., 2004: A fossil origin for the magnetic fields in A stars and white dwarfs. *Nature*, **431**, 819–821.
- Braithwaite, J. & Spruit, H. C., 2006: A differential rotation driven dynamo in a stably stratified star. *Astron. Astrophys.*, submitted. Available at astro-ph/0509693 and at www.mpa-garching.mpg.de/~henk/dynamo.pdf
- Brun, A. S. & Zahn, J.-P., 2006: Magnetic confinement of the solar tachocline. *Astron. Astrophys.*, submitted.
- Charbonneau, P. & MacGregor, K. B., 1993: Angular momentum transport in

- magnetized stellar radiative zones. II. The solar spin-down. *Ap. J.* **417**, 762–780. [CM93]
- Christensen-Dalsgaard, J., Gough, D. O. & Thompson, M. J., 1992: On the rate of destruction of lithium in late-type main-sequence stars. *Astron. Astrophys.*, **264**, 518–528.
- Elliott, J. R. & Gough, D. O., 1999. Calibration of the thickness of the solar tachocline. *Ap. J.*, **516**, 475–481.
- Fricke, K., 1969: Stability of rotating stars II: the influence of toroidal and poloidal magnetic fields. *Astron. Astrophys.*, **1**, 388–398.
- Garaud, P., 2002: Dynamics of the solar tachocline – I. An incompressible study. *Mon. Not. Roy. Astron. Soc.*, **329**, 1–17.
- Gilman, P. A. & Miesch, M. S., 2004: Limits to penetration of meridional circulation below the solar convection zone. *Ap. J.*, **611**, 568–574. [GMi]
- Gough, D. O. & McIntyre, M. E., 1998. Inevitability of a magnetic field in the Sun’s radiative interior. *Nature*, **394**, 755–757. [GM98]
- Haynes, P. H., *et al.*, 1991: On the “downward control” of extratropical diabatic circulations by eddy-induced mean zonal forces. *J. Atmos. Sci.*, **48**, 651–678. Also **53**, 2105–2107.
- Manney, G. L., *et al.*, 1994: On the motion of air through the stratospheric polar vortex. *J. Atmos. Sci.*, **51**, 2973–2994 (Upper Atmosphere Research Satellite special issue).
- McIntyre, M. E., 1994. The quasi-biennial oscillation (QBO): some points about the terrestrial QBO and the possibility of related phenomena in the solar interior. In *The Solar Engine and its Influence on the Terrestrial Atmosphere and Climate* (Vol. **25** of NATO ASI Subseries I, Global Environmental Change), ed. E. Nesme-Ribes; Heidelberg, Springer, 293–320.
- McIntyre, M. E., 2003a. Solar tachocline dynamics: eddy viscosity, anti-friction, or something in between? In *Stellar Astrophysical Fluid Dynamics*, ed. M.J. Thompson & J. Christensen-Dalsgaard. Cambridge, University Press, 111–130.
- McIntyre, M. E., 2003b. On global-scale atmospheric circulations. In *Perspectives in Fluid Dynamics: A Collective Introduction to Current Research*, ed. G. K. Batchelor, H. K. Moffatt, M. G. Worster; Cambridge, University Press, 631 pp., 557–624. Paperback edition, with corrections.
- Mestel, L. & Weiss, N. O., 1987: Magnetic fields and non-uniform rotation in stellar radiative zones. *Mon. Not. Roy. Astron. Soc.*, **226**, 123–135.
- Riese, M., *et al.*, 2002. Stratospheric transport by planetary wave mixing as observed during CRISTA-2. *J. Geophys. Res.*, **107** (D23), paper no. 8179, doi:10.1029/2001JD000629.
- Spiegel, E. A. & Zahn, J.-P., 1992. The solar tachocline. *Astron. Astrophys.*, **265**, 106–114.
- Spruit, H. C., 1999: Differential rotation and magnetic fields in stellar interiors. *Astron. Astrophys.*, **349**, 189–202. [S99]
- Spruit, H. C., 2002. Dynamo action by differential rotation in a stably stratified stellar interior. *Astron. Astrophys.*, **381**, 923–932. [S02]
- Townsend, A. A., 1958: The effects of radiative transfer on turbulent flow of a stratified fluid. *J. Fluid Mech.*, **4**, 361–375.
- Zahn, J.-P., 1974: Rotational instabilities and stellar evolution. In *Stellar Instability and Evolution*, ed. P. Ledoux *et al.*. Dordrecht, Reidel, 185–195.